Bioorganic & Medicinal Chemistry Letters 20 (2010) 5521–5526

Contents lists available at ScienceDirect

Bioorganic & Medicinal Chemistry Letters

journal homepage: www.elsevier.com/locate/bmcl

Synthesis of MRI contrast agents derived from DOTAM-Gly-L-Phe-OH incorporating a disulfide bridge: Conjugation to a cell penetrating peptide and preparation of a dimeric agent

Mojmír Suchý [a,b], Alex X. Li [b], Robert Bartha [b], Robert H. E. Hudson [a,*]

[a] Department of Chemistry, The University of Western Ontario, London, ON, Canada N6A 5B7
[b] Centre for Functional and Metabolic Mapping, Robarts Research Institute, The University of Western Ontario, London, ON, Canada N6A 5K8

ARTICLE INFO

Article history:
Received 6 May 2010
Revised 15 July 2010
Accepted 16 July 2010
Available online 23 July 2010

Keywords:
PARACEST
Europium
Contrast agent
TAT
Bimetallic

ABSTRACT

A cell penetrating peptide conjugate and dimeric PARACEST MRI contrast agents, based on the DOTAM-Gly-L-Phe-OH scaffold have been prepared in moderate yields using diethyl azodicarboxylate (DEAD) or iodine-mediated disulfide bridge formation as a key step. Magnetic (PARACEST) properties of these agents have been evaluated.

Magnetic resonance imaging (MRI) represents an important diagnostic tool widely employed to obtain anatomical images of soft tissues based upon the detection of protons in the body.[1] Gd^{3+}-based T_1-shortening MRI contrast agents (CAs) are prominently used in clinical diagnostics and decrease bulk water relaxation time constants through the rapid exchange of agent-bound water with bulk water. However, there are several limitations associated with their current use. Firstly, their presence is always detected in an MR image; and secondly, designing Gd^{3+}-compounds sensitive to metabolic or environmental conditions that maintain rapid water exchange and consequently high relaxivity is difficult.

Recently, an alternative method of generating contrast in MRI was introduced based on chemical exchange saturation transfer (CEST).[2] Subsequently, a large number of paramagnetic ion-containing lanthanide(III) complexes, mainly involving Eu^{3+} and Tm^{3+}, have been prepared which are capable of inducing large hyperfine shifts of coordinated water protons as well as other exchangeable protons present in close proximity to the metal center.[3] The term PARACEST MRI CAs has been coined to describe these molecules.[4] When compared to classical Gd^{3+}-derived MRI CAs, the spectrum of information obtained using PARACEST MRI CAs is potentially broader as the CEST effect is sensitive to the environment. PARACEST CAs have been previously used to detect physiological conditions such as tissue temperature[5] and pH.[6] Primary metabolites such as glucose,[7] polyarginine[8] and lactate[9] can also be detected, along with biologically important phosphate anions[10] and Zn^{2+} cations.[11] PARACEST MRI CAs have been successfully applied toward the detection of enzymatic activities, for example: cathepsin D;[12] β-galactosidase;[13] caspase-3;[14] or urokinase plasminogen activator.[15]

Despite the number of PARACEST MRI contrast agents recently described, their detection in vivo[16] remains a challenging task. This can be attributed to rather low sensitivity as well as limited bioavailability of these agents. To address these issues, we turned our attention to a sulfanyl (thiol, SH) modified ligand **1** (Fig. 1),[17] based on Eu^{3+} DOTAM-Gly-Phe-OH (**2b**, Fig. 1),[18] a DOTAM-polyamide based PARACEST MRI CA exhibiting a high level of sensitivity within the physiological temperature range (36–40 °C). To facilitate the vectorization of **2b** and increase its bioavailability, thiol **1** was conjugated to a cell penetrating TAT peptide[19] by diethylazodicarboxylate (DEAD)-promoted disulfide bond formation[20] followed by metalation with $EuCl_3 \cdot 6H_2O$. The resulting conjugate (**3**, Fig. 1) is expected to undergo reductive disulfide cleavage by endogenous thiols, such as glutathione, within the intracellular compartment leaving the Eu^{3+} containing reporter group trapped inside the cells for an extended period of time. Alternatively, treatment with an exogenous thiol may facilitate excretion after a period of MR imaging.[21]

Disulfide linkages have been employed previously in the preparation of macromolecular complexes and peptide conjugates,

* Corresponding author. Fax: +1 519 661 3022.
E-mail address: rhhudson@uwo.ca (R.H.E. Hudson).

0960-894X/$ - see front matter © 2010 Elsevier Ltd. All rights reserved.
doi:10.1016/j.bmcl.2010.07.070

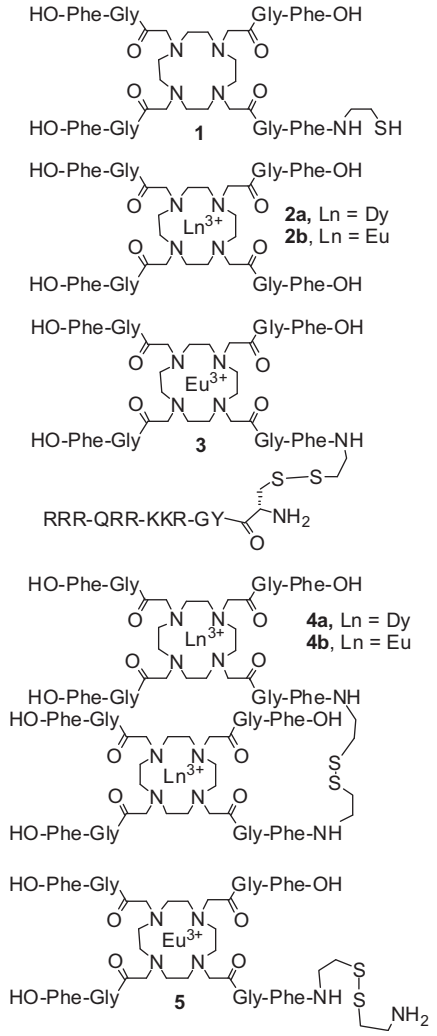

Figure 1. Structures of ligands and complexes **1**–**5.**

although disulfide bond formation was not always the key step. For instance, an approach using cystamine as a linker wherein the β-amino group was used for amide bond formation has been described for the conjugation of Gd^{3+}-derived MRI CAs with poly(L-glutamic acid)[21] and poly(L-arginine).[22] A Gd^{3+}-based DOTA has been conjugated to reduced bovine serum albumin (BSA) or silica nanoparticles by disufides formed through an intermediate methanethiosulfonate derivative.[23] Also carbon–sulfur bond formation was exploited when a sulfanyl modified DOTA ligand was attached to phosphopeptides by Michael addition to dehydroalaninyl or β-methyldehydroalaninyl residues.[24]

The presence of a free SH group in **1** also prompted us to explore the preparation of a homodimeric ligand via symmetrical disulfide bond formation. The resulting bifunctional disulfide-bridged ligand was envisioned to undergo a double metalation with Dy^{3+} or Eu^{3+} salts to form a bimetallic PARACEST MRI CAs **4a**,**b** (Fig. 1) expected to possess higher sensitivity, compared to monometallic CAs **2**, based on literature precedent. Sherry and co-workers used free-radical polymerization and prepared a series of DOTAM-based linear polymers which upon metalation with Eu^{3+} salts afforded PARACEST MRI CAs with enhanced sensitivities.[25] A large number of PARACEST CAs have also been shown to be conjugated to adenovirus, although diminished viral bioactivity was observed when the number of ligands attached to the virus exceeded ~1000.[26] Several dendritic pH responsive multimeric PARACEST MRI CAs have been synthesized and have been shown to retain sensitivity on a per-lanthanide basis.[27] PANAM-based dendritic PARACEST CAs have been prepared and used to detect flank tumor in vivo.[16a,28] Morrow and co-workers have evaluated Eu^{3+}- and Nd^{3+}-based bimetallic complexes consisting of two DOTAM units joined by *p*-dibenzyl linkage as potential carbonate or DNA responsive PARACEST MRI CAs.[29] We have recently prepared and evaluated both homo- (containing two Eu^{3+}) and heterobimetallic (containing Eu^{3+} and Tm^{3+}) complexes featuring two different chelator subunits.[30]

In the present study, we report the synthesis and magnetic properties associated with cell penetrating peptide conjugated PARACEST MRI CA **3** and bimetallic complexes **4** (Fig. 1). The synthetic methodology represents an alternative approach to conjugation of DOTA- and DOTAM-derived ligands with peptides that rely mainly on amide bond formation between DOTA- or DOTAM-derived carboxylic acids and N-terminus unprotected peptides attached to a solid support.[31]

Sulfanyl-modified ligand **1** has been prepared following the experimental protocol recently established in our laboratory.[17] We initially attempted to conjugate ligand **1** to the cell penetrating TAT peptide ('*N*'-YG-RKK-RRQ-RRR-'*C*') by solid phase peptide synthesis. The fully protected peptide (for the protecting groups see ref.32) attached to Wang's resin was derivatized with commercially available Fmoc-Cys(Mmt)-OH. The acid labile Mmt protecting group was selectively removed (1% TFA in CH_2Cl_2), followed by treatment with ligand **1** preactivated with diethylazodicarboxylate (DEAD).[20] Cleavage of the peptide from the resin (5% TES in wet TFA) followed by HPLC purification afforded the desired disulfide-bridged conjugate in unacceptable (<5%, based on ligand **1**) yield, despite many attempts to modify the reaction conditions. To overcome this problem we turned to solution phase conjugation chemistry as indicated in Scheme 1.[33] Thus, Fmoc-Cys(Trt)-OH (**6**) was coupled (HBTU, DIPEA, and DMF) to the resin bound, fully protected peptide **7**. Peptide **8** was obtained after cleavage from the resin and HPLC purification (Scheme 1). Treatment of peptide **8** with ligand **1** under the conditions of DEAD-promoted asymmetrical disulfide bond formation afforded conjugate **9** in 27% yield (based on **1**) after HPLC purification. With ligand **9** in hand we performed the metalation with $EuCl_3{\cdot}6H_2O$ (Scheme 1). This reaction was found to be surprisingly slow, requiring large excess of the Eu^{3+} salt (20 equiv), elevated reaction temperature (60 °C) and prolonged reaction time (2–3 days). A time course study of the metalation of **9** with $EuCl_3{\cdot}6H_2O$ can be found in Supplementary data. HPLC purification afforded desired Eu^{3+} DOTAM-Gly-L-Phe-OH-TAT peptide conjugate **3** in 65% yield (Scheme 1). It is worth

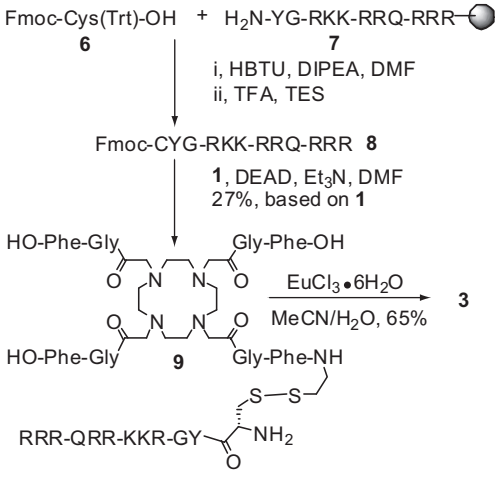

Scheme 1. Synthesis of Eu^{3+} DOTAM-Gly-L-Phe-OH peptide conjugate **3**.

pointing out, that excess $EuCl_3 \cdot 6H_2O$ was efficiently removed by HPLC as confirmed by Xylenol Orange test.[34] The resulting peptide conjugate was characterized by ESI-HRMS.[33]

Synthesis of CAs **4a**,**b** was accomplished as depicted in Scheme 2.[35] DEAD-promoted oxidation of **1** was found to produce multiple products and was therefore abandoned. However, thiol **1** smoothly underwent disulfide formation upon treatment with Br_2 or I_2 in the presence of Et_3N and the reaction was further optimized using I_2 as an oxidizing agent. The presence of the disulfide **10** as a major product was confirmed by UPLC-ESI-HRMS.[35] Fortunately, no HPLC purification of crude disulfide **10** was required at this stage. The crude disulfide **10** was subjected to metalation with $EuCl_3 \cdot 6H_2O$ (Scheme 2). Similar to the metalation of conjugate **9**, a large excess of $EuCl_3 \cdot 6H_2O$ (20 equiv), prolonged reaction time and elevated temperature (4–5 days at 70 °C) was required to achieve the metalation of **10**. The desired product, PARACEST MRI CA **4b** was isolated by semi-preparative HPLC (Fig. 2) in 30% yield (based on **1**) and was characterized by ESI-HRMS.[35] The Dy^{3+} based CA **4a** was prepared (in 36% yield based on **1**) similarly (Scheme 2) by treatment with $DyCl_3 \cdot 6H_2O$. The excess Ln^{3+} salts were efficiently removed during the HPLC purification. The absence of free Ln^{3+} in CAs **4** was verified using a Xylenol Orange test.[34]

After the desired contrast agents were prepared, we evaluated their PARACEST properties. Peptide conjugate **3** is expected to undergo an intracellular reduction of the disulfide bond mediated by the thiols normally present within the body (e.g., glutathione). The actual CA trapped within an intracellular environment would therefore be an Eu^{3+}-derived complex of **1**. We have previously shown,[17] that synthesis of such complex is troublesome due to the oxidation during the treatment with $EuCl_3 \cdot 6H_2O$. In Ref.17 we used a model compound, complex **5** (Fig. 1) possessing a protected SH group and were able to determine its PARACEST properties. The CEST effect due to bound water (ca. 45 ppm) was found to be slightly lower (ca. 35% at 10 mM) compared to parent CA **2b**.[17] Considering our plans to use the peptide conjugate **3** as biocompatible temperature probe for MRI, we have also established the relationship between the temperature and the chemical shift of bound water in complex **5**. As observed for the unmodified parent compound **2b**, a linear relationship within the physiological temperature range was obtained as depicted in Supplementary data.

Due to the presence of two lanthanide(III) metals in CAs **4**, they were expected to posses higher sensitivity compared to parent monomeric structures **2**. A PARACEST effect (<5% at ca. −750 ppm)

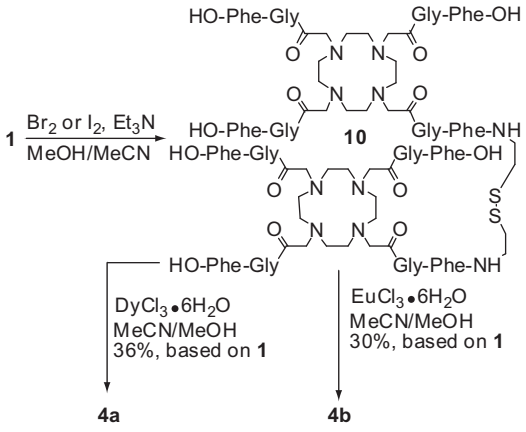

Scheme 2. Synthesis of dimeric PARACEST MRI CAs **4**.

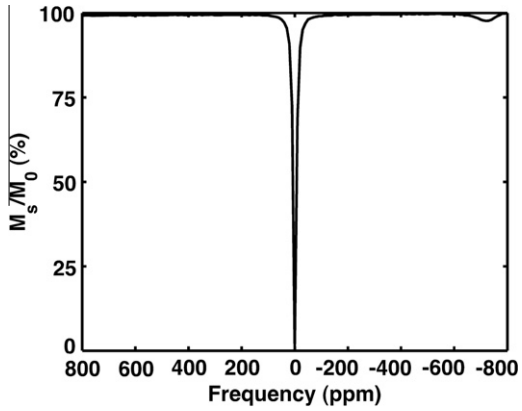

Figure 2. CEST spectrum of 4**a** (23.4 mM in water containing 20% MeCN, room temperature, saturation power B_1 30 μT, presaturation time TS 3.9 s).

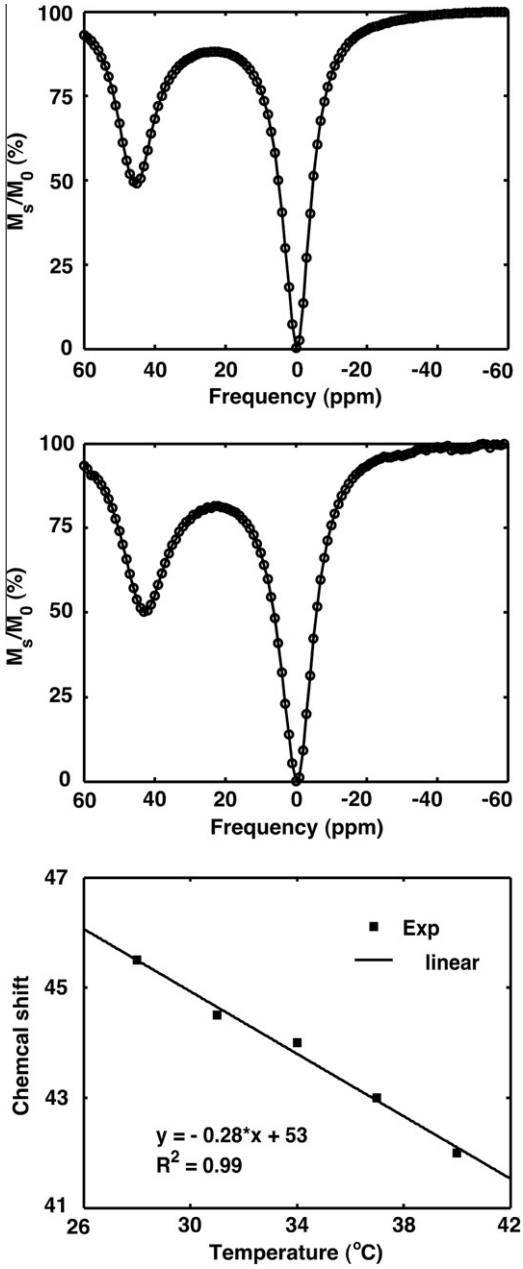

Figure 3. CEST spectra of the bimetallic PARACEST MRI CA **4b** at two temperatures (10 mM) at 28 °C (top) and 37 °C (middle) and the dependence of the bound water chemical shift on temperature (bottom).

due to bound water[3a] was observed in the corresponding spectrum (at 23.4 mM) of Dy^{3+} derived dimer **4a** (Fig. 2). This observation is consistent with the results obtained for Dy^{3+} DOTAM.[3a] Due to the fact, that peaks associated with bound water in complexes **2a** (see Supplementary data) and **4a** (Fig. 2) are rather broad, it was difficult to establish a relationship between the number of Dy^{3+} centers and the PARACEST signal. It appears that more than two Dy^{3+} centers will be required to create a PARACEST MRI CA with enough sensitivity for in vivo applications. The experimental conditions used to acquire the CEST spectrum of **4a** would indeed preclude any in vivo study.

To obtain basic information about the sensitivity of **4b**, its CEST spectrum (at 10 mM) was acquired at 28 °C and 37 °C (Fig. 3). A strong (>50%) CEST effect due to bound water present in the coordination sphere of **4**[3a] was observed. Since the CEST effect of CA **2b** acquired under identical experimental conditions[18b] is smaller (ca. 40%), the increase in the saturation transfer is attributed to the presence of the additional paramagnetic Eu^{3+}. CA **4b** is not completely soluble in water at 10 mM, therefore an addition of MeCN (20%) was necessary to solubilize it completely. As discussed below no MeCN was required at concentrations of 1 mM or lower. To rule out the possibility that the presence of MeCN affected the magnetic properties of CA **4b**, CEST spectra of the original monometallic CA **2b**[18] were also acquired in water and in water containing 20% MeCN at 10 mM concentration. These results confirmed that the presence of MeCN had a negligible effect on the overall detection sensitivity of CA **1**. This observation is consistent with literature reports wherein it is accepted practice to use MeCN to solubilize PARACEST CAs for in vitro characterization.[36]

With the intention to use the bimetallic CA **4b** for MRI based temperature mapping, the correlation between the temperature and chemical shift was established. The CEST spectra of **4b** (at 10 mM concentration, temperature range 28–40 °C) in water containing 20% MeCN were acquired using previously established experimental conditions[18b] (pH 7.0, B_0 9.4 T, B_1 14 μT, saturation time 10 s). There was a linear correlation between the temperature and the chemical shift of the bound water pool in the CEST spectrum, Figure 3.

Previously developed temperature responsive PARACEST MRI CAs suffer from low sensitivities. The required high concentration of CA will likely be incompatible with in vivo studies. In order to further elucidate the detection sensitivity of CA **4b**, we measured its CEST spectra at low concentrations (1 and 0.5 mM, at 37 °C) and compared them to those of CA **2b** under identical conditions, Figure 4. It is important to point out, that the addition of MeCN was not required to achieve these low concentrations. Both agents were found to exhibit the CEST effect due to bound water present in their coordination spheres. Interestingly, the CEST effect observed with dimeric CA **4b** was found to be about 1.6 times greater (13% vs 8% at 1 mM; 6% vs 3.6% at 0.5 mM) than the CEST effect observed with CA **2b**. The increased sensitivity correlates with the number of Eu^{3+} cations present in the molecule, whilst maintaining the desirable temperature dependent properties. It is reasonable to expect a less than twofold increase in the CEST effect when comparing **2b** and **4b**. Several factors may generally result in a lower than expected increase in CEST effect including altered T1 relaxation, altered exchange rates, the nonlinear nature of the concentration dependence of the CEST effect at high concentrations, and the expected less than unity proportionality of the CEST effect with concentration at low concentrations.[37] Although changes in T_1 relaxation induced by the agent are likely not a factor for the Eu(III)

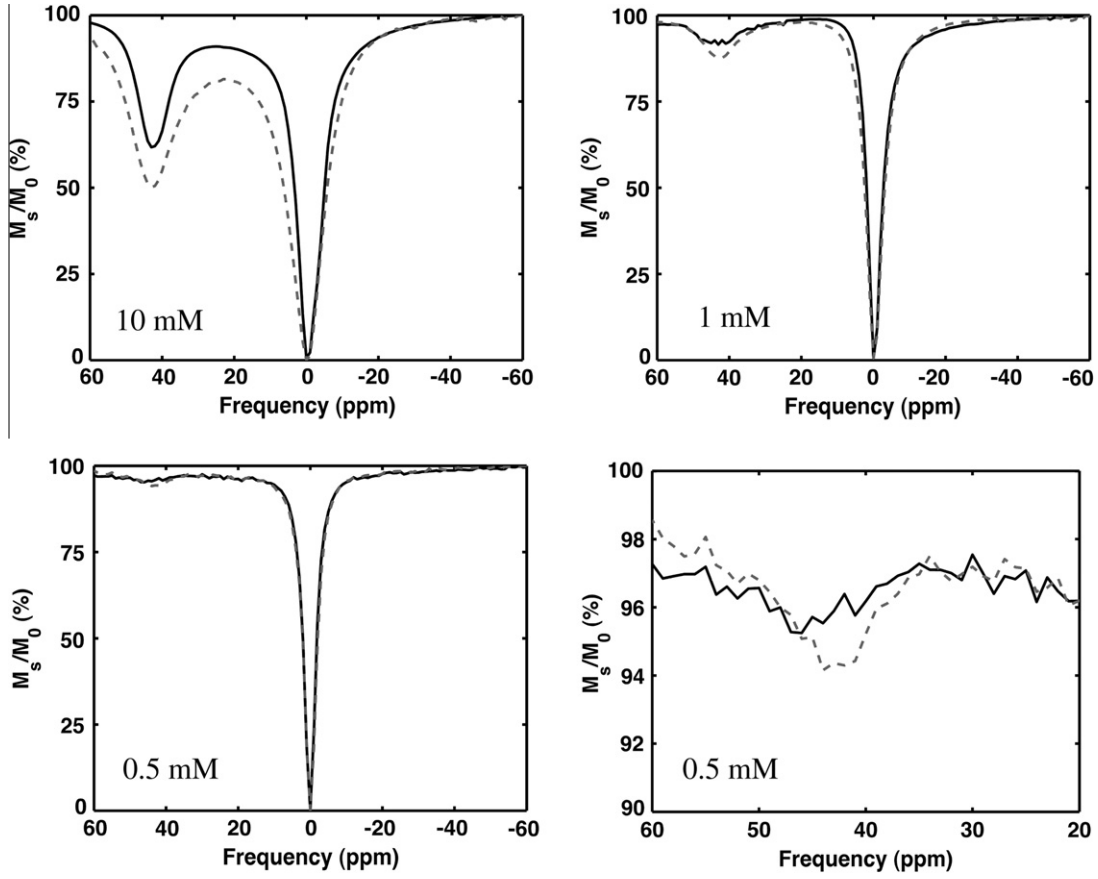

Figure 4. Comparison of the monomeric (**2b**) and dimeric europium-containing compounds (**4b**). CEST spectra (at 37 °C) of CAs **2b** (solid line) and **4b** (dashed line) at 10 mM (top left); 1 mM (bottom left) and 0.5 mM (top right). Expanded CEST spectrum at 0.5 mM (bottom right).

based compounds, particularly at the low concentrations used in the current study, the other mechanisms may each contribute to some extent.

In summary we have shown, that sulfanyl modified ligand **1** can be used as a starting material for the synthesis of peptide conjugated as well as dimeric PARACEST MRI CAs based on a DOTAM-Gly-L-Phe-OH scaffold. A linear correlation between the temperature and the chemical shift of bound water was observed with model complex **5** and dimeric Eu^{3+}-based complex **4b**. Considering the significant increase in sensitivity of CA **4b** compared to the monomeric structures **2b** and **5**, this compound may be useful for the purpose of temperature mapping. The increase of sensitivity in the case of Dy^{3+} derived dimer **4a** is modest, indicating that more than two metal centers are required to boost the sensitivity in to a practically useful range. Studies on cellular uptake of CA **3** are currently in progress and will be reported in due course.

Acknowledgment

The authors thank the Ontario Institute for Cancer Research (OICR) for the financial support of this work.

Supplementary data

Supplementary data associated with this article can be found, in the online version, at doi:10.1016/j.bmcl.2010.07.070.

References and notes

1. For the recent reviews on MRI CAs see: (a) Yoo, B.; Pagel, M. D. *Front. Biosci.* **2008**, *13*, 1733; (b) Geraldes, C. F. G. C.; Laurent, S. *Contrast Med. Mol. Imaging* **2009**, *4*, 1; (c) Kubíček, V.; Tóth, É.. In *Advances in Inorganic Chemistry*; Elsevier Academic Press: San Diego, 2009; Vol. 61; (d) Terreno, E.; Delli Castelli, D.; Viale, A.; Aime, S. *Chem. Rev.* **2010**, *110*, 3019.
2. For the seminal paper introducing this idea see: Ward, K. M.; Aletras, A. H.; Balaban, R. S. *J. Magn. Reson.* **2000**, *143*, 79.
3. For the recent reviews on PARACEST MRI CAs see: (a) Woods, M.; Woessner, D. E.; Sherry, A. D. *Chem. Soc. Rev.* **2006**, *35*, 500; (b) Sherry, A. D.; Woods, M. *Annu. Rev. Biomed. Eng.* **2008**, *10*, 391; (c) Terreno, E.; Delli Castelli, D.; Aime, S. *Contrast Med. Mol. Imaging* **2010**, *5*, 78; (d) Wu, Y.; Evbuomwan, M.; Melendez, M.; Opina, A.; Sherry, A. D. *Future Med. Chem.* **2010**, *2*, 351; (e) Viswanathan, S.; Kovács, Z.; Green, K. N.; Ratnakar, S. J.; Sherry, A. D. *Chem. Rev.* **2010**, *110*, 2960.
4. Zhang, R. S.; Merrit, M.; Woessner, D. E.; Lenkinski, R.; Sherry, A. D. *Acc. Chem. Res.* **2003**, *36*, 783.
5. (a) Terreno, E.; Delli Castelli, D.; Cravotto, G.; Milone, L.; Aime, S. *Invest. Radiol.* **2004**, *39*, 235; (b) Zhang, S.; Malloy, C. R.; Sherry, A. D. *J. Am. Chem. Soc.* **2005**, *127*, 17572.
6. (a) Aime, S.; Delli Castelli, D.; Terreno, E. *Angew. Chem., Int. Ed.* **2002**, *41*, 4334; (b) Aime, S.; Barge, A.; Delli Castelli, D.; Fedeli, F.; Mortilarro, A.; Nielsen, F. U.; Terreno, E. *Magn. Reson. Med.* **2002**, *47*, 639.
7. (a) Zhang, S.; Trokowski, R.; Sherry, A. D. *J. Am. Chem. Soc.* **2003**, *125*, 15288; (b) Trokowski, R.; Zhang, S.; Sherry, A. D. *Bioconjugate Chem.* **2004**, *15*, 1431.
8. Aime, S.; Delli Castelli, D.; Terreno, E. *Angew. Chem., Int. Ed.* **2003**, *42*, 4527.
9. Aime, S.; Delli Castelli, D.; Fedeli, F.; Terreno, E. *J. Am. Chem. Soc.* **2002**, *124*, 9364.
10. Huang, C. H.; Morrow, J. R. *J. Am. Chem. Soc.* **2009**, *131*, 4206.
11. Trokowski, R.; Ren, J.; Kalman, F. K.; Sherry, A. D. *Angew. Chem., Int. Ed.* **2005**, *44*, 6920.
12. Suchý, M.; Ta, R.; Li, A. X.; Wojciechowski, F.; Pasternak, S. H.; Bartha, R.; Hudson, R. H. E. *Org. Biomol. Chem.* **2010**, *8*, 2560.
13. Chauvin, T.; Durand, P.; Bernier, M.; Meudal, H.; Doan, B. T.; Noury, F.; Badet, B.; Beloeil, J. C.; Tóth, É. *Angew. Chem., Int. Ed.* **2008**, *47*, 4370.
14. (a) Yoo, B.; Pagel, M. D. *J. Am. Chem. Soc.* **2006**, *128*, 14032; (b) Yoo, B.; Raam, M. S.; Rosenblum, R. M.; Pagel, M. D. *Contrast Med. Mol. Imaging* **2007**, *2*, 189.
15. Yoo, B.; Sheth, V. R.; Pagel, M. D. *Tetrahedron Lett.* **2009**, *50*, 4459.
16. (a) Ali, M. M.; Liu, G.; Shah, T.; Flask, C. A.; Pagel, M. D. *Acc. Chem. Res.* **2009**, *42*, 915. and references cited therein.; For the recent example from our laboratory see: (b) Jones, C. K.; Li, A. X.; Suchý, M.; Hudson, R. H. E.; Menon, R. S.; Bartha, R. *Magn. Reson. Med.* **2010**, *63*, 1184.
17. Suchý, M.; Li, A. X.; Bartha, R.; Hudson, R. H. E. *Org. Biomol. Chem.* **2008**, *6*, 3588.
18. (a) Wojciechowski, F.; Suchý, M.; Li, A. X.; Azab, H. A.; Bartha, R.; Hudson, R. H. E. *Bioconjugate Chem.* **2007**, *18*, 1625; (b) Li, A. X.; Wojciechowski, F.; Suchý, M.; Jones, C. K.; Hudson, R. H. E.; Menon, R. S.; Bartha, R. *Magn. Reson. Med.* **2008**, *59*, 374.
19. For the recent review on the use of cell penetrating peptides in drug delivery see: Stewart, K. M.; Horton, K. L.; Kelly, S. O. *Org. Biomol. Chem.* **2008**, *6*, 2242.
20. For the recent review on disulfide bond formation see: Witt, D. *Synthesis* **2008**, 2491.
21. Lu, Z. R.; Wang, X.; Parker, D. L.; Goodrich, K. C.; Buswell, H. R. *Bioconjugate Chem.* **2003**, *14*, 715.
22. Major, J. L.; Meade, T. J. *Acc. Chem. Res* **2009**, *42*, 893. and references cited therein.
23. Thonon, D.; Jacques, V.; Desreux, J. F. *Contrast Med. Mol. Imaging* **2007**, *2*, 24.
24. Mattila, K.; Siltainsuu, J.; Balaspiri, L.; Ora, M.; Lönnberg, H. *Org. Biomol. Chem.* **2005**, *3*, 3039.
25. Wu, Y.; Zhou, Y.; Ouari, O.; Woods, M.; Zhao, P.; Soesbe, T. C.; Kiefer, G. E.; Sherry, A. D. *J. Am. Chem. Soc.* **2008**, *130*, 13854.
26. Vasalaitiy, O.; Gerard, R. G.; Zhao, P.; Sun, X.; Sherry, A. D. *Bioconjugate Chem.* **2008**, *19*, 598.
27. Pikkemaat, J. A.; Wegh, R. T.; Lamerichs, R.; van de Molengraaf, R. A.; Langereis, S.; Burdinski, D.; Raymond, A. Y. F.; Jansse, H. M.; de Waal, B. F. M.; Willard, N. P.; Meijer, E. W.; Grüll, H. *Contrast Med. Mol. Imaging* **2007**, *2*, 229.
28. Ali, M. M.; Yoo, B.; Pagel, M. D. *Mol. Pharm.* **2009**, *6*, 1409.
29. Nwe, K.; Andolina, C. M.; Huang, C. H.; Morrow, J. R. *Bioconjugate Chem.* **2009**, *20*, 1375.
30. Suchý, M.; Li, A. X.; Bartha, R.; Hudson, R. H. E. *Tetrahedron Lett.* **2010**, *51*, 1087.
31. For the recent review on conjugation of DOTA-derived ligands with peptides see: De León-Rodríguez, L. M.; Kovacs, Z. *Bioconjugate Chem.* **2008**, *19*, 391.
32. *General experimental procedures:* All reagents were commercially available, unless otherwise stated. Protected peptide **7** (protecting groups R-Pbf, Q-Trt, K-Boc, Y-*t*Bu, '*N*'-terminal Fmoc) attached to Wang's resin was custom synthesized. All solvents were HPLC grade and used as such, except for water (18.2 M Ω cm millipore water). Solvents were removed under reduced pressure in a rotary evaporator. Aqueous solutions were lyophilized. HPLC analysis and purification was carried out using a radial compression module C18 300 Å column (particle size 15 μm; 8 × 100 mm cartridge) monitored by a diode array detector (wavelength range 190–600 nm). Mobile phase: Method A: 90% H_2O/10% MeCN—100% MeCN over 20 min, linear gradient, flow rate 3 mL/min. UPLC analysis was carried out using a C18 column (particle size 1.7 μm; 2.1 i.d. × 50 mm) and monitored by a diode array (wavelength range 190–600 nm) and HR-ESI-TOF-MS detectors. Mobile phase: Method B: 100% H_2O—25% H_2O/75% MeCN over 3 min, linear gradient, flow rate 0.25 mL/min; mass spectra (MS) were obtained on TOF mass spectrometer, using electron spray (ESI) for ionization. CEST spectra associated with CAs **4** and **5** have been acquired on 400 MHz (9.4 T) NMR spectrometer in water or in 80% water/20% MeCN as described previously.[18b] Temperature was controlled by blowing warm air over each phantom using a small animal monitoring and gating system and monitored using a fibre optic probe placed in a separate adjacent phantom.
33. *Synthesis of Eu^{3+} DOTAM-Gly-L-Phe-OH peptide conjugate* **3**: In a manual peptide synthesis vessel, resin (150 mg) containing the protected peptide (**7**, 7.62×10^{-5} mol) was treated with 20% piperidine in DMF (2 mL, repeated twice) for 5 min. The resin was consecutively washed with dry DMF and CH_2Cl_2 (ca. 2 × 10 mL each, repeated twice). In a separate vial DIPEA (110 μL, 6.30×10^{-4} mol) and HBTU (107 mg, 2.84×10^{-4} mol) were added to a cooled (0 °C) solution of Fmoc-Cys(Trt)-OH (**6**, 185 mg, 3.15×10^{-4} mol) in DMF (700 μL). The resulting mixture was added (after 10 min at 0 °C) to the washed resin in a peptide vessel followed by agitation for 1.5 hour at rt. The resin was washed as described above and was treated with cleavage cocktail (5 mL, for 1.5 h at rt) prepared by dissolving water (300 μL) and TES (200 μL) in TFA (10 mL). The TFA solution was concentrated to ca. 10% of its original volume, was cooled to 0 °C, cold (−20 °C) Et_2O (20 mL) was added and the mixture was set aside for 1 h at −20 °C. The resulting mixture was transferred to centrifuge tubes, was centrifuged (1000 rpm for 3 min), the supernatant was decanted and the pellet was dissolved in water (3 mL). The aqueous solution thus obtained was lyophilized to afford 54 mg of the crude Fmoc-CYG-RKK-RRQ-RRR. This material was purified by semi-preparative HPLC (Method A),[32] fractions were concentrated to leave the peptide **8** (25.8 mg, 19%) as colorless solid; HPLC: t_R 8.0 min. A stock solution of diethylazodicarboxylate (DEAD, 0.1 M) was prepared by dissolving DEAD (16 μl) in dry DMF (1 ml). DEAD solution in DMF (0.1 M, 14.4 μl, 1.44×10^{-5} mol) was added to a centrifuge tube containing dry DMF (100 μl), followed by the addition of Et_3N (40 μl, 2.88×10^{-4} mol) and cooling to 0 °C. In a separate Eppendorf tube sulfanyl modified DOTAM-Gly-Phe-OH **1** (18.4 mg, 1.44×10^{-5} mol) was dissolved in dry DMF (350 μl) and the solution obtained was added dropwise (over 2 min, with stirring) to a previously prepared DEAD and Et_3N solution (kept at 0 °C). The ice bath was removed and stirring continued for 10 min at rt after which time the mixture obtained was then transferred to another centrifuge tube containing peptide **8** (25.8 mg, 1.44×10^{-5} mol). The resulting suspension was stirred for 48 h at rt, then it was diluted with water (ca. 4 ml) and finally lyophilized to afford 32 mg of the residue. This residue was purified by semi-preparative HPLC (Method A),[32] fractions were concentrated to leave DOTAM-Gly-Phe-TAT disulfide conjugate **9** (11.2 mg, 27%) as colorless solid; HPLC: t_R 7.9 min. HRMS (ESI) *m*/*z*: found 2940.5361 $[M+H]^+$ (2940.5215 calcd for $C_{129}H_{203}N_{46}O_{30}S_2$). $EuCl_3 \cdot 6H_2O$ (41 mg, 1.12×10^{-4} mol) was added to a solution of DOTAM-Gly-Phe-TAT disulfide conjugate **9** (16.5 mg, 5.60×10^{-6} mol) in water (1 ml). The mixture was incubated for 72 h at 60 °C, then cooled to rt and was subjected for purification by semi-preparative HPLC (Method A),[32] fractions were concentrated to leave Eu^{3+} DOTAM-Gly-Phe-TAT disulfide conjugate **3** (11.2 mg, 65%) as colorless solid; HPLC: t_R 7.8 min. HRMS (ESI) *m*/*z*: found 3090.4192 $[M-2H]^+$ (3090.4068 calcd for $C_{129}H_{200}N_{46}O_{30}S_2Eu$).

34. Barge, A.; Cravotto, G.; Gianolio, E.; Fedeli, F. *Contrast Med. Mol. Imaging* **2006**, *1*, 184–188.
35. *Synthesis of dimeric PARACEST MRI CAs* **4**: Et_3N (7 μl, 5.00×10^{-5} mol) was added to a solution of sulfanyl modified DOTAM-Gly-Phe-OH **1** (32 mg, 2.50×10^{-5} mol) in MeOH (1 ml) and the mixture was cooled to 0 °C. A solution (0.1 M in MeCN) of I_2 (250 μl, 2.50×10^{-5} mol) was added dropwise (over 2 min) with stirring, the stirring continued for 10 min at 0 °C and then for 48 h at rt. Solvent was evaporated and crude DOTAM-Gly-Phe-OH derived symmetrical disulfide dimer **10** was used for the metalation without further purification. Its presence was confirmed by UPLC analysis as described in Ref.[32]; HRMS (ESI) *m*/*z*: found 2558.1382 $[M+H]^+$ (2558.1313 calcd for $C_{124}H_{161}N_{26}O_{30}S_2$). Crude dimer **10** was slowly (ca. 4 h required) dissolved in water (1.5 ml at 70 °C with stirring). $EuCl_3{\cdot}6H_2O$ (183 mg, 5.00×10^{-4} mol) or $DyCl_3{\cdot}6H_2O$ (188 mg, 5.00×10^{-4} mol) were added to separate reaction mixtures, followed by the addition of MeCN (600 μl) and stirring for 120 h at 70 °C.
Dy^{3+} DOTAM-Gly-Phe-OH derived symmetrical disulfide dimer **4a** was purified by semi-preparative HPLC (Method A),[32] fractions were concentrated to leave colorless solid (13.6 mg, 38%); HPLC: t_R 16.6 min. HRMS (ESI) *m*/*z*: found 2877.9750 $[M-2H]^+$ (2877.9696 calcd for $C_{124}H_{159}N_{26}O_{30}S_2Dy_2$).
Eu^{3+} DOTAM-Gly-Phe-OH derived symmetrical disulfide dimer **4b** was purified by semi-preparative HPLC (Method A),[32] fractions were concentrated to leave colorless solid (10.8 mg, 30%); HPLC: t_R 10.1 min. HRMS (ESI) *m*/*z*: found 2856.9219 $[M-4H]^+$ (2856.9190 calcd for $C_{124}H_{154}N_{26}O_{30}S_2Eu_2$).
36. (a) Woods, M.; Woessner, D. E.; Zhao, P.; Pasha, A.; Yang, M. Y.; Huang, C. H.; Vasalitiy, O.; Morrow, J. R.; Sherry, D. A. *J. Am. Chem. Soc.* **2006**, *128*, 10155; (b) Huang, C. H.; Morrow, J. R. *Inorg. Chem.* **2009**, *48*, 7237.
37. Woessner, D. E.; Zhang, S.; Merritt, M. E.; Sherry, A. D. *Magn. Reson. Med.* **2005**, *53*, 790.